Experimental development and bond graph dynamic modeling of a Brazed Plate Heat Exchanger (BPHE).

Mohamed Kebdani*
Ecole Centrale de Lille,
CS 20048, 59651 Villeneuve d'Ascq. France.
Email : kebdani.mp@hotmail.fr
*****Corresponding author.

Geneviève Dauphin-Tanguy
Ecole Centrale de Lille,
CRIStAL UMR CNRS 9189,
CS 20048, 59651 Villeneuve d'Ascq. France.
Email : genevieve.dauphin-tanguy@ec-lille.fr

Antoine Dazin
Arts et Métiers Paris Tech/ LML UMR CNRS 8107,
Boulevard Louis XIV, 59000 Lille. France.
Email : antoine.dazin@ensam.eu

P. Dupont
Ecole Centrale de Lille/LML UMR CNRS 8107,
CS 20048, 59651 Villeneuve d'Ascq. France.
Email : patrick.dupont@ec-lille.fr

Abstract
This article is devoted to the dynamic study of a brazed plate heat exchanger (BPHE). First, is proposed an introduction to the industrial context of the current FUI THERMOFLUIDE project. A succinct presentation of the heat exchanger technology is proposed. Afterward, is given a state of the art about BPHEs modeling, heat transfer and pressure drop correlations. Then a detailed mathematical description of an original dynamic model is presented. The last section deals with a description of the experimental test rig and performed validation tests.

Keywords: Brazed plate heat exchanger; bond graph methodology; dynamic; transient; single-phase flow; heat transfer correlations, modeling.

Nomenclature

c_p	Specific heat	$J/kg\cdot K$	λ	thermal conductivity	$W/m\cdot K$
D_h	Hydraulic diameter	m	μ	dynamic viscosity	$Pa\cdot s$
D_p	Port diameter	m	ρ	density	kg/m^3
e	wall thickness	m	β	Chevron angle	degre
G	Flow density	W	f	Friction coefficient	---
h	Convection coefficient		Φ	Heat flow	J/s
H	Latent heat of condensation	J/kg	0	initial state	
$\dot{H}$	flow enthalpy	J/s	acc	accumulation	
g	acceleration of gravity	m	amb	ambient	
l	Plate Width	m	col	Colector	
L	Channels lengt	m	$conv$	Convection	
m	mass	kg	dis	Distributor	
$\dot{m}$	Mass flow rate	kg/s	$fric$	Friction	
N_{can}	Channels number	---	in	inlet	
N_t	Number of plates	---	$grav$	gravity	
Nu	Nusselt number	---	liq	liquid	
P	Pressure	Pa	out	outlet	
p	corrugation depth	m	Per	perimiter	

p_{co}	Pitch of corrugation	m	Δ	difference
Pr	Prandtl number	---	PC	Primary circuit
Re	Reynolds number	---	SC	Secondary circuit
S	Surface	m^2	LMTD	Logarithmic mean temperature difference
t	time	s	Wall	Exchanger wall
T	Temperature	K		

1 INTRODUCTION AND STATE OF THE ART

During their functioning, electronic components dissipate, by Joule effect, significant thermal flows. Furthermore, if ever this heat is not correctly managed, temperature of the electronic devices increases, until exceeding the junction temperature which leads them to a complete dysfunction. Several solutions have been proposed to prevent the damage of power components and make them functioning in some optimal conditions.

The choice of the 13 companies involved in the current project has been oriented towards 2-Phases Loop Mechanically Pumped **(2-PLMP).** Such systems are undoubtedly the most efficient in terms of heat transfer (Kebdani et al. 2015), (Lachassagne 2010) and (Serin 2007) . Indeed, in addition to their architectural flexibility and compactness, they guarantee appropriate cooling using a pump. The Figure 1 shows a 2-PLMP composed of an evaporator, a heat exchanger, pipes, a pump and a pressurizer whose an advanced dynamic bond graph model is proposed by (Kazuhiro et al. 2015) and (Matías et al. 2015).

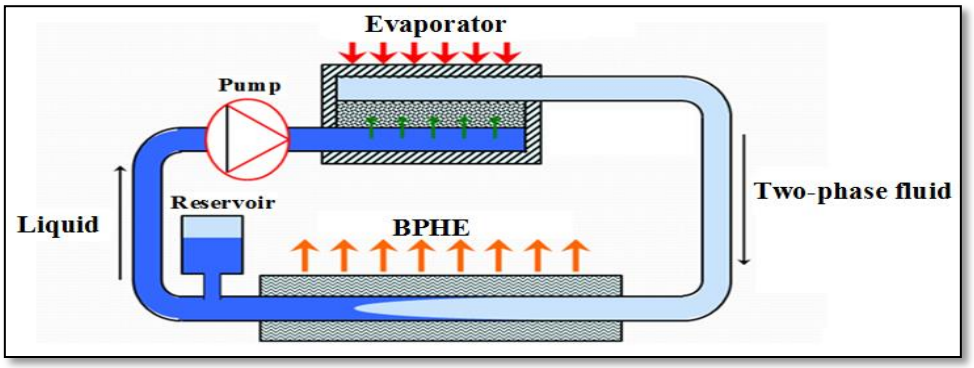

Figure 1 : Design of Mechanically Pumped Loops (2-PLMP).

A 2-PLMP is a closed loop containing a refrigerant fluid moved by a pump. The electronic component is positioned just above the evaporator (hot source) see Figure 1. The heat flow emitted is transferred simultaneously by conduction and convection phenomena to the working fluid, which makes its temperature increasing. The stored enthalpy is consequently transferred from the evaporator to the brazed plate heat exchanger (BPHE) where the hot fluid is cooled and even sub-cooled releasing thereby its specific heat to a cold source. Such fluidic loops are very promising and constitute the heart of our research work. (Kebdani et al. 2015).

The component studied in this article is the BPHE. Actually, various heat exchanger technologies exist; the choice depends on the nature of the application. For instance, radiators and BPHE are often selected in space activities; for land-based applications (automotive, rail...) an air exchanger with air cross-flow may be adequate.
As regards to our project, the BPHE chosen here is named SWEP with reference "B5Tx6", see Figure 2.

1.1 Technology and advantages of BPHE

The BPHE is built as a stack of corrugated plates. The set of thermal plates is brazed with copper. Also, the heat exchanger is composed of a number of connections called “ports”, positioned at the corners / edges of the cover plates, see Figure 2. During the brazing operation, the copper is melted and perfectly leads to connection points between plates, forming thereby a unique functional monobloc. This process ensures a high level of impermeability and guarantees a structural integrity which allows BPHE to withstand important operating pressures, up to 45 *bar*.

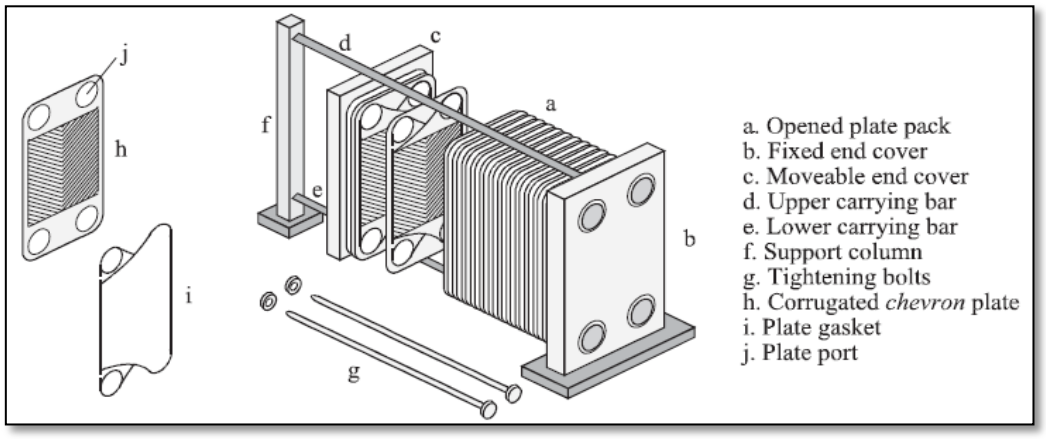

Figure 2: Design of the heat exchanger, exploded view of a BPHE.

The type of the flow pattern adopted in this work is a counter-current. The two refrigerants flow in opposite directions, as shown schematically in Figure 3 (a). Actually, this configuration promotes better heat exchanges, compared to performance provided by a co-current heat exchanger. Indeed, in this interesting configuration, it is proven (using Logarithmic Mean Temperature Difference (LMTD) method and under certain conditions) that the outlet temperature of the working fluid T_{out_PC} may be lower than the outlet temperature of the secondary fluid T_{out_SC}, as shown in Figure 3 (b), which is impossible with an anti- methodical (co-current) exchanger.

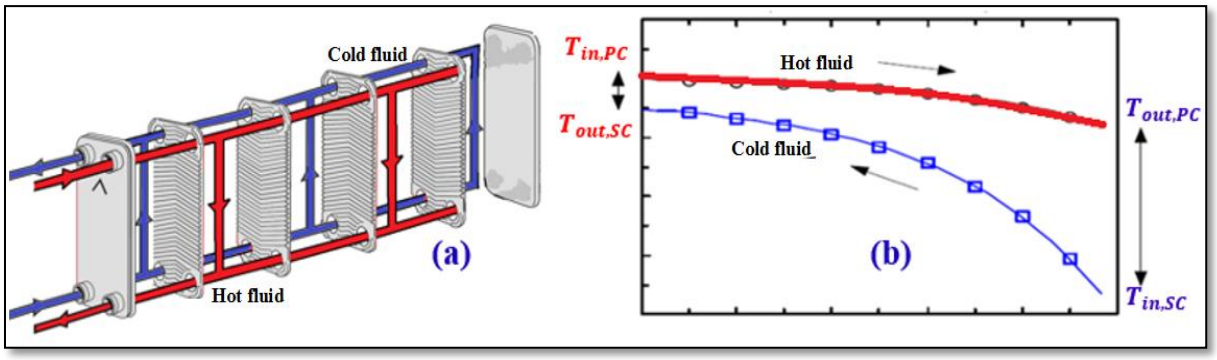

Figure 3 : (a) Flow directions in a counter-current BPHE.
(b) Spatial evolution of the temperature of cold and hot fluids in a counter-current BPHE.

BPHE provides a number of outstanding benefits. Known for their reduced compactness (ratio of exchange surface to the total volume), they may exist with a volume 20 to 30% less than that one of a tubular heat exchanger (Eldeeb et al. 2014) and (Thermofin 2010). Also, channel design provides effective heat transfers. Actually, the multiple fluid streams intersect at the

central channel, inducing a complex turbulent flow (Maqbool 2012) and (Muthuraman 2011), which promotes great heat transfers (Lorenzo et al. 2012)**,** (Eldeeb et al. 2014). Furthermore, turbulence and secondary flows developed in the exchanger inhibit the formation of fouling layers. For more details see (Eldeeb et al. 2014).

BPHE is used in a wide range of applications: air conditioning, refrigeration, food and chemical industry. This component has shown its worth in monophasic and biphasic applications. References (Eldeeb et al. 2014), (Muthuraman 2011), (Gullapalli 2013) and (Vlasogiannis et al. 2002) contain more details about the different uses of the so called BPHE.

1.2 State of the art on BPHE modeling

Unlike tubular heat exchangers, nowadays the scientific literature identifies very few modeling works specific to BPHE (Taborek 1992). On the other side, the vast majority of disclosed research works give a summary exposition of mean calculation axes. Important details are not always available. *As to* BPHE *models based on bond graph methodology, they absolutely don't exist in the open literature.* The literature survey shows that the dynamic modeling efforts are mainly proprietary of some manufacturers and are so confidential (Kakac & Liu 1998).

a) Examples of some modeling works related to BPHEs

- Method of (Arman & Rabas 1995):

Arman and Rabas developed a **stationary model**, able to predict the thermo hydraulic state of the coolant. The BPHE iterative model is based on an incremental procedure.

- Model of (Gut et al. 2004):

Gut presents an algorithm that allows the simulation of flow in the **steady state**. The algorithm uses the resolution of energy conservation equation, and is based on the following assumptions:

1. The model treats only steady states.
2. No heat loss to the outside is considered.
3. The author does not deal with the phase change problems.
4. The overall heat transfer coefficient is meant to be constant.
5. Finally, the flow is assumed to be "plug" along the exchanger.

- Model of (Medjaher et al. 2009): Pseudo bond graph of a tubular heat exchanger

Medjaher publishes a **dynamic model**. It is the only known model based on bond graph methodology. Its complexity is declared to be of medium level. However, let's precise that the modeled heat exchanger is not a BPHE, but composed of a simple single U-shaped tube, which contains a coolant fluid as shown in Figure 4. The assumptions are:

1. Absence of non-condensable gas.
2. The liquid phase is incompressible.
3. The heat exchanger is perfectly adiabatic.
4. The usual Nusselt's assumptions are included.
5. The heat exchanger is fed with pure steam in the saturation state.

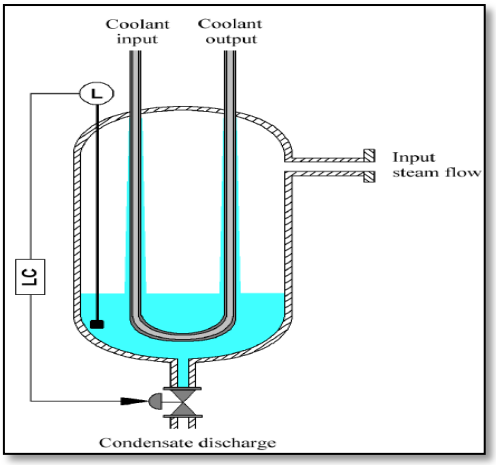

Figure 4 : Schema of the heat exchanger modeled by Medjaher (Medjaher et al. 2009).

Mass and energy conservation equations are solved systematically in the primary circuit divided in two control volumes: pure steam, and liquid volume. Also, the resolution of the energy conservation equation is performed in two other control volumes: the secondary fluid and the tube wall. The temperature variation along the wall is calculated by dividing the wall into small segments.

- Model of (Sotoodeh et al. 2015) :

The objective function is to investigate the geometries that give best heat recovery or higher cold stream outlet terminal temperature. The design parameters include number of constructs and geometric variables of each construct. The constructal heat exchanger volume and heat transfer area are kept constant and equal to the volume and heat transfer area of the optimized ordinary heat exchanger. The optimization of the study case reveals higher heat recovery in constructal plate-fin heat exchanger in comparison with ordinary plate-fin heat exchanger.

b) Synthesis of literature revue and scientific contributions

The literature revue leads us to draw up a synthetic and comparative Table 1 which is supposed to position better the originality of the new proposed BPHE model.

property	**Arman** (Arman & Rabas 1995)	**Gute** (Gut et al. 2004)	**Medjaher** (Medjaher et al. 2009)	**Kebdani (current article)**
Single phase flow		✓		✓
dynamic study			✓	✓
bond graph approach			✓	✓
sensitivity of the thermo physical properties to the pressure and temperature	✓		✓	✓
Heat loss to the ambient				✓
longitudinal conduction			✓	✓
heat transfer coefficient correlations				✓
Pressure drop correlations				✓

Table 1: Literature revue and comparison between BPHE models.

1.3 State of the art on the thermal convection coefficients specific to BPHEs

One of the major problems encountered when modeling the BPHE, are the right correlation of the convection coefficient in both primary and secondary circuits of the exchanger, and the calculation of the pressure drop. Today, there is no universal and reliable correlation. The reason is due to the strong dependence of heat transfer phenomena of many parameters such as: plate geometry, thermo-physical property of the fluid, void fraction, pressure and

temperature, Reynolds (laminar or turbulent), without forgetting the dependence on the pattern flow.

The literature provides access to a wide range of correlations whose number exceeds one hundred. Wang (Wang et al. 2007) and Ayub (Ayub 2003) propose a summary work of existing correlations. Below is proposed some correlations valid for water in monophasic state. Keep in mind that each correlation remains closely linked to the operating conditions under which it was developed.

First, the evaluation of such exchanger's performance needs the development of specific experimental methods giving access to predictions of the exchange coefficient and pressure drops. In this context, various authors conducted different studies of BPHE instrumentation and flow visualization:

- There have been attempts based on the observation of flows (Vlasogiannis et al. 2002), (Volker & Kabelac 2010) for a BPHE composed of a single channel and built with a transparent plate. Consequently a flow pattern map is drawn.

- More recently (Freund & Kabelac 2010) have developed an experimental technique based on infrared visualization, to characterize the spatial distribution of the convective heat exchange coefficient for a single-phase flow (water).

- (Rong et al. 1995) declare that it is possible to estimate theoretically the performance of a BPHE operating in single phase with water as refrigerant fluid. The final results of their work show that it would be appropriate to utilize correlations of pressure drop and heat transfer that take into account corrugation chevron angles.

Among the numerous available correlations, the following, are selected (table. 2):

<table>
<tr><th>Author</th><th>Reference</th><th>comments</th><th>formula</th></tr>
<tr><td>Heavner</td><td>(Gullapalli 2013)</td><td>Valid for water.</td><td>$J = \frac{Nu}{\Pr^{1/3}.\left(\frac{\mu}{\mu_{wall}}\right)^{0.17}} = b \cdot \mathrm{Re}^{m}$ and $h_{conv} = \frac{Nu \cdot \lambda}{D_h}$
<table>
<tr><th>Chevron Angle Combination</th><th>Mean Chevron Angle</th><th>a</th><th>n</th><th>b</th><th>m</th></tr>
<tr><td>45°/0°</td><td>22.5°</td><td>1.715</td><td>0.0838</td><td>0.278</td><td>0.683</td></tr>
<tr><td>67°/0°</td><td>33.5°</td><td>1.645</td><td>0.1353</td><td>0.308</td><td>0.667</td></tr>
<tr><td>45°/45°</td><td>45°</td><td>0.810</td><td>0.1405</td><td>0.195</td><td>0.692</td></tr>
<tr><td>67°/45°</td><td>56°</td><td>0.649</td><td>0.1555</td><td>0.118</td><td>0.720</td></tr>
<tr><td>67°/67°</td><td>67°</td><td>0.571</td><td>0.1814</td><td>0.089</td><td>0.718</td></tr>
</table></td></tr>
<tr><td>Boyko and Kruzhilin</td><td></td><td>Valid for water.</td><td>$h_{conv} = 0.0021 \cdot \mathrm{Re}_{liq}^{0.8} \cdot \mathrm{Pr}_{liq}^{0.43} \cdot \left(\frac{\lambda_{liq}}{D_h}\right)$</td></tr>
<tr><td>Muley and Manglik</td><td>(Longo 2009)</td><td>Valid for water.
$\mathrm{Pr}_{eau} \in [5;10]$
$\mathrm{Re}_{eau} \in [200;1200]$</td><td>$h_{conv} = 0.277 \cdot \left(\frac{\lambda_{liq}}{D_h}\right) \cdot \mathrm{Re}_{liq}^{0.766} \cdot \mathrm{Pr}_{liq}^{0.333}$</td></tr>
<tr><td>Kim</td><td>(Muthuraman 2011)</td><td>Valid for water.</td><td>$h_{conv} = 0.295 \cdot \left(\frac{\lambda_{liq}}{D_h}\right) \cdot \mathrm{Re}^{0.64} \cdot \mathrm{Pr}^{0.32} \cdot \left(\frac{\pi}{2} - \beta\right)^{0.09}$</td></tr>
<tr><td>Alpha laval</td><td></td><td>Valid for water.</td><td>$Nu = 234 \cdot \lambda_{liq} \cdot \mathrm{Pr}^{1/3} \cdot \left[\frac{\rho_{liq} \cdot \Delta P}{\mu_{liq}}\right]^{0.3274}$ and $h_{conv} = \frac{Nu \cdot \lambda}{D_h}$</td></tr>
</table>

Table 2 : Summary correlations of thermal convection coefficients used for single-phase flow.

1.4 State of the art on the friction coefficients related to BPHEs

The pressure losses inside a BPHE are generally the sum of three contributions:
• Pressure variation due to gravitation.
• Pressure drops at ports.
• Pressure drops due to wall friction.

This section aims to present the pressure losses correlations.

a) Pressure variation due to gravitation.

The change in pressure due to gravity is determined by the hydrostatic equation

$$\Delta P_{grav} = \pm \rho_{liq} \cdot g \cdot L \quad \textbf{(1)}$$

b) Pressure drop in distributors and collectors "ports".

The losses generated inside distributors (inflow) and collectors (outflow) are empirically estimated by Shah and Focke (Longo 2009) and (Focke W.W., Zachariades J. 1985) :

$$\Delta P_{col/dis} = \frac{1.5 \cdot G^2}{2 \cdot \rho_{liq}} \quad \textbf{(2)}$$

c) Pressure losses due to friction

The friction coefficient is very complicated to determine. The Table 3 shows a number of correlations available in the literature.

Author	Reference	comments	formula
Muley and Manglik	(Gullapalli 2013)	Valid for water. For a Prandtl : $\mathrm{Pr} \in [2.4;4.5]$	*For* $\mathrm{Re} \in [2;200]$ $f = \left[\left(\frac{40.32}{\mathrm{Re}} \right)^5 + \left(\frac{8.12}{\mathrm{Re}^{-0.5}} \right)^5 \right]^{-0.2}$ *For* $\mathrm{Re} \geq 1000$ $f = 1.274 \cdot \mathrm{Re}^{-0.15}$
Heavner	(Gullapalli 2013)	Valid for water	$f = a \cdot \mathrm{Re}^{-n}$

Chevron Angle Combination	*Mean Chevron Angle*	*a*	*n*
45°/0°	22.5°	1.715	0.0838
67°/0°	33.5°	1.645	0.1353
45°/45°	45°	0.810	0.1405
67°/45°	56°	0.649	0.1555
67°/67°	67°	0.571	0.1814

Darcy Weisbach		Valid for water	Hagen- Poiseuille for laminar flow $f = \frac{64}{\mathrm{Re}}$ Blasius for turbulent flow $f = \frac{0.3164}{\mathrm{Re}^{0.25}}$

Table 3 : Summary of friction coefficient correlations used for single-phase flow.

2 DESCRIPTION OF THE BPHE DYNAMIC MODEL

2.1 Assumptions and contributions

The model is based on the following hypotheses:

1. The fluid is unidirectional.
2. The fluid is supposed to be constantly monophasic liquid.
3. The fluid in the secondary circuit (SC) flows with a constant mass flow rate.
4. The device is not perfectly insulated from the ambient, and then thermal exchanges with the exterior are modeled using specific correlations.
5. The refrigerant used for the simulation is water, while the validation tests are performed with water containing 4% of PAG (lubrication oil).
6. Primary circuit (PC) and secondary circuit (CS) of the BPHE are modeled by means of finite volumes where physical quantities are supposed to be homogeneous (lumped parameters model).

Main contributions

Based on the comparison with the existing modeling works, and according to the synthesis given in Table 1, the contributions are multiple:

1. The use of bond graph tool for the development of a dynamic model is the first novelty. Note that, no BPHE model based on this approach is nowadays published in the scientific literature.

The modularity of the bond graph methodology meets with a reasonable level of accuracy when it comes to discuss the compromise between precision and efficiency. Actually, it is always possible to enrich the model by incorporating other phenomena without changing its original structure (towards a better accuracy).

2. The proposed model is designed to handle the dynamic behavior, unlike the vast majority of models limited to steady state.

3. The transitional model pays particular attention to the multiple thermal convection coefficients governing transfers of heat flow.

The novelty, compared to previous works, is twofold. First, convection coefficients are variable, changing with the evolution of local thermodynamic conditions. Second, the thermal behavior of the heat exchanger is experimentally validated without any use of recalibration or adjustment of the set of these coefficients. This means that the model is quite robust and autonomous.

4. Unlike most existing models, the proposed model takes into account the heat exchange with the outside. Also, the longitudinal conduction along the walls is modeled.

5. Gaussian and polynomial correlations of thermo physical properties are specially developed on the basis of data provided by the National Institute of Standards and Technology (NIST) [site1].

2.2 Volume discretization of the exchanger

A BPHE is constituted of a multitude of channels in both circuits: hot (PC), and cold (SC), as is visible in Figure 5. However, in the current work, the exchanger is considered as the union of four control volumes, detailed in Figure 6:

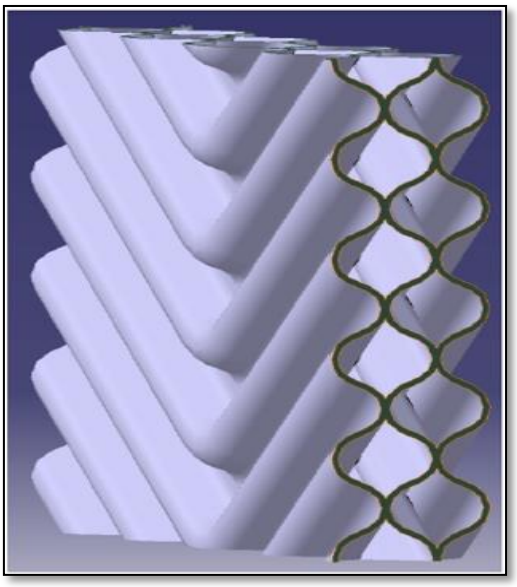

Figure 5: Internal geometry of a BPHE.

- Primary circuit (PC), is assimilated to a simple pipe: volume V1.
- Secondary circuit (SC), also cylindrical, contains water in single phase state. This circuit is represented by one volume V2 as shown in Figure 6.
- Exchange wall between the PC and SC is represented by the volume V3,
- Exchange wall between the SC and the ambient is represented by the volume V4.

2.3 General structure of the bond graph model

The structure of the BPHE bond graph model is shown in Figure 7.

⇨ Physical description :

➢ The four sub models shown in Figure 6 refer to the four volumes represented by the following bond graph elements :

Volume	designation	Bond graph element
V1	primary circuit	RC elements with 2 thermal ports
V2	secondary circuit	RC elements with 2 ports (thermal and hydraulic).
V4	exchange wall between the SC and the ambient	C element with 1 port (thermal).

➢ The network drawn with dotted lines corresponds to the hydraulic part of the condenser, while the continuous lines represent the thermal part of the exchanger.

➢ All treated heat transfer phenomena (convection and conduction) are modeled by dissipative elements, noted: R in bond graph theory. The Figure 6 gives precise idea about the distribution of various thermal exchanges included in the bond graph model.

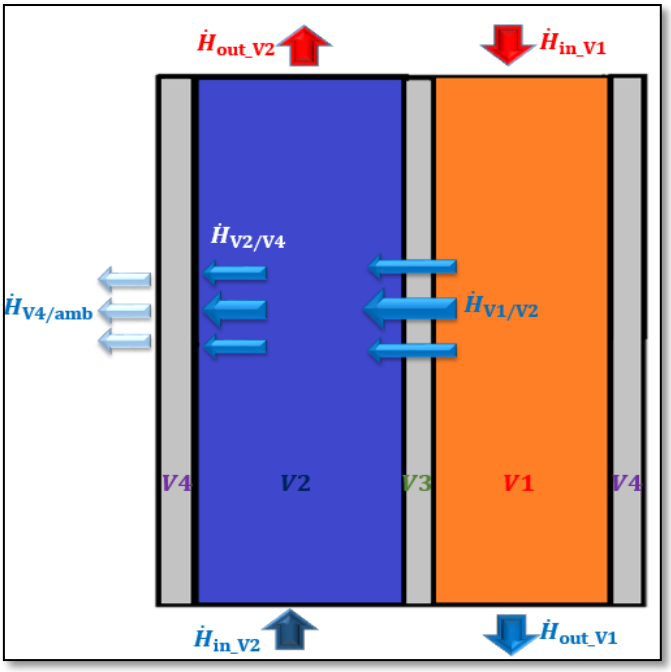

Figure 6: Volume discretization of the BPHE, and distribution of heat flows occurring during the cooling phenomenon.

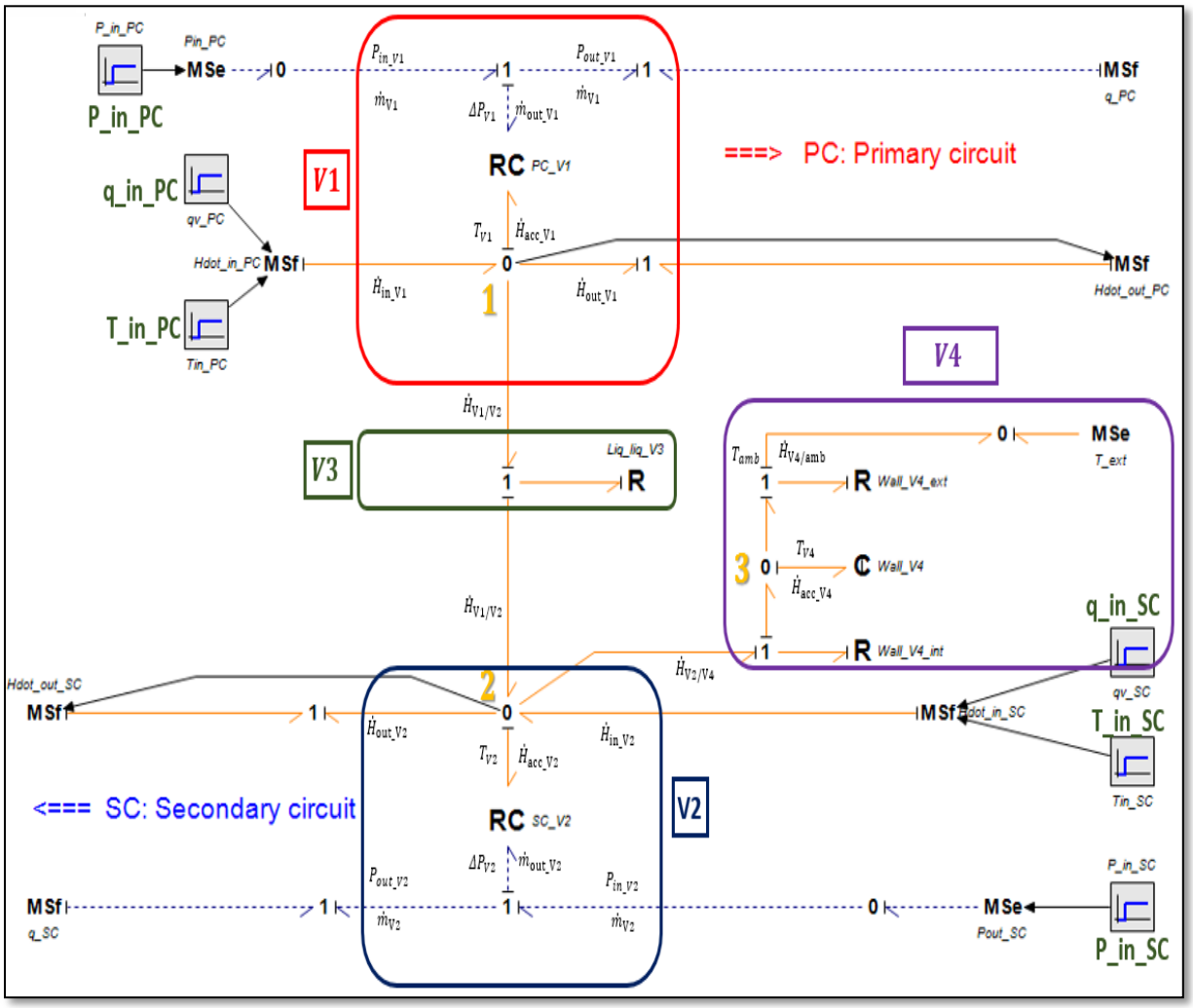

Figure 7 : Dynamic bond graph model of the BPHE.

2.4 Description of the dynamic bond graph model

Now is presented a succinct description of conservation equations (mass and energy) governing the thermal-hydraulic behavior of the flow inside the BPHE. The resolution of equations is ensured by Runge-Kutta method which is integrated in 20Sim.

The "effort / flow" variables are:

- Hydraulic part: Pressure and mass flow rate.
- Thermal part: Temperature and enthalpy flow rate (in case of convection) or heat flow rate (for conduction).

The developed model is called a "pseudo bond graph" and is shown Figure 7.
Interpolations giving the evolution of thermo physical properties are specifically developed for the current project with accuracy care, and are presented in our article (Kebdani et al. 2015).

a) Volumes V1 and V2 of the primary and secondary circuits
The mathematical formalism for calculating the fluid temperature in the two volumes V1 and V2 is the same.

The temperature $T_{V1}(t)$ of the fluid crossing the volume $V1$ (PC) is calculated using the energy balance. Furthermore, the fluid inside $V1$ receives three thermal flows :

- $\dot{H}_{in\_V1}$ modeled in bond graph by the element $MSf_{Hdot\_in\_PC}$.
- $\dot{H}_{out\_V1}$ modeled by the element $MSf_{Hdot\_out\_PC}$.
- $\dot{H}_{V1/V2}$ modeled by the element $R_{Liq\_liq\_V3}$.

⇨ The energy balance is written in the junctions 0_t numbered 1 In the Figure 7:

$$\dot{H}_{acc\_V1} = \dot{H}_{in\_V1} - \dot{H}_{V1/V2} - \dot{H}_{out\_V1} \quad \textbf{(3)}$$

⇨ The enthalpy stored inside $V1$ is then calculated in the element RC_{PC_V1} as follows:

$$H_{acc\_V1}(t) = \int_t \dot{H}_{acc\_V1}(t)dt + H_{V1,0} \quad \textbf{(4)}$$

where, $H_{V1,0}$ is the initial enthalpy in $V1$.

⇨ The constitutive law of the element RC_{PC_V1} giving the temperature of the fluid is then:

$$T_{V1}(t) = \frac{H_{acc\_V1}(t)}{m_{V1}.c_{p,V1}} \quad \textbf{(5)}$$

⇨ The pressure drop ΔP_{V1} calculated in the 2-ports element RC_{PC_V1} is obtained using the equations: **(6)**, **(7)**, **(8)** and **(9)** discussed in detail in section (1.4). For frictional pressure losses induced in single phase flow ΔP_{fric} the formula of Darcy- Weisbach is used.

$$\Delta P_{V1} = \Delta P_{grav} + \Delta P_{fric} + \Delta P_{col/dis} \quad \textbf{(6)}$$

where :

$$\Delta P_{grav} = \rho_{liq\_V1} \cdot g \cdot L_{V1} \quad \textbf{(7)}$$

$$\Delta P_{col/dis} = \frac{1.5 \cdot G^2}{2 \cdot \rho_m} \quad \textbf{(8)}$$

$$\Delta P_{fric} = \frac{1}{2} \cdot \rho_{liq\_V1} \cdot v^2 \cdot \frac{L_{V1}}{D_h} \cdot f = 2 \cdot \frac{\dot{m}^2_{in\_V1}}{\rho_{liq\_V1} \cdot \pi^2 \cdot D_h^3} \cdot f \quad \textbf{(9)}$$

$\Delta P_{col/dis}$ represents the pressure losses in the collector and the distributor of the condenser.
If : $\mathrm{Re} < 100$ (laminar regime according to Wanniarachchi (Muthuraman 2011)), then Hagen-Poiseuille formula is used:

$$f = \frac{64}{\mathrm{Re}} \quad \textbf{(10)}$$

Otherwise (transient or turbulent regime), the formula of Blasius for turbulent flow regime gives:

$$f = \frac{0.3164}{\mathrm{Re}^{0.25}} \quad \textbf{(11)}$$

Now it remains to determine the hydraulic diameter: D_h. For a better understanding of the geometrical problem, quantities used in the formula **(12**) are reported in Figure 8:

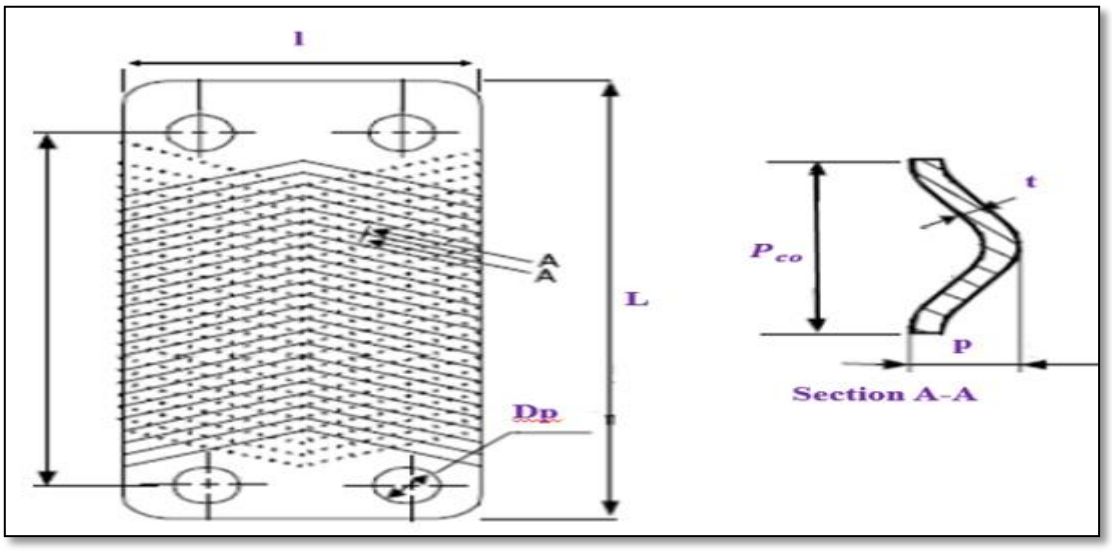

Figure 8: Distribution of geometric parameters on the thermal plate of a BPHE.

$$D_h = \frac{4 \cdot S_{V1}}{Per_{V1}} = \frac{4 \cdot b \cdot l}{2 \cdot l \cdot \Phi} = \frac{2 \cdot b}{\Phi} \quad \textbf{(12)}$$

where :

- $\Phi = 1.17$, a value given by the manufacturer SWEP
- $b = p - t$. Where p is the corrugation depth, t: corrugation thickness.

b) Volume V4 constituting the exchange wall between the SC and the ambient.
The temperature $T_{V4}(t)$ of the wall separating the SC from the ambient is calculated using the energy balance. Note that the heat exchanges between the volume V4 and its surrounding are mainly due to two thermal flows, as shown in Figure 6. The flows are:

- $\dot{H}_{V2/V4}$ and $\dot{H}_{V4/amb}$

⇨ The energy balance is written in the junction 0_t numbered 3, see Figure 7**Erreur ! Source du renvoi introuvable.**:

$$\dot{H}_{acc\_V4} = \dot{H}_{V1/V4} - \dot{H}_{V4/amb} \quad \textbf{(13)}$$

⇨ The enthalpy stored inside $V4$ is then calculated in the element C_{Wall_V4} as follows:

$$H_{acc\_V4}(t) = \int_t \dot{H}_{acc\_V4}(t)dt + H_{V4,0} \quad \textbf{(14)}$$

where, $H_{V4,0}$ is the initial enthalpy in $V4$.

⇨ The constitutive law of the thermal element C_{Wall_V4} giving the wall temperature is then:

$$T_{V4}(t) = \frac{H_{acc\_V4}(t)}{m_{V4}.c_{p,V4}} \quad \textbf{(15)}$$

2.5 Expression of convective flows

Heat flows due to convection phenomenon are modeled using dissipative element R, and are summarized below in tables 4 and 5. According to Newton, convection happening close to the walls is given by:

$$\dot{H} = h_{conv} \cdot S_{exch} \cdot \Delta T \quad \textbf{(16)}$$

BG element	**heat flow:** $\dot{H}$	**Convection coefficient** h_{conv}	**Exchange surface** S_{exch}	ΔT
$R_{Liq\_liq\_V3}$	$\dot{H}_{V1/V2}$	$h_{conv} = \frac{1}{\frac{e_{wall}}{\lambda_{wall}} + \frac{1}{h_{V1}} + \frac{1}{h_{V2}}}$ • **Boyko et Kruzhilin :** $h_{V1} = 0.021 \cdot \mathrm{Re}_{V1}^{0.8} \cdot \mathrm{Pr}_{V1}^{0.43} \cdot \left(\frac{\lambda_{liq}}{D_h}\right)$ • **Alfa Laval :** $h_{V2} = 234 \cdot \lambda_{liq} \cdot \mathrm{Pr}_{liq}^{1/3} \cdot \left[\frac{\rho_{liq} \cdot \Delta P_{V2}}{\mu_{liq}}\right]^{0.3274}$	$S_{exch} = 0.0240.m^2$ Value given by the manufacturer SWEP	$T_{V1} - T_{V2}$
$R_{Wall\_V4\_int}$	$\dot{H}_{V2/V4}$	• **Alfa Laval :** $h_{conv} = 234 \cdot \lambda_{liq} \cdot \mathrm{Pr}_{liq}^{1/3} \cdot \left[\frac{\rho_{liq} \cdot \Delta P_{V2}}{\mu_{liq}}\right]^{0.3274}$	$S_{exch} = 0.001.m^2$	$T_{V2} - T_{V4}$
$R_{Wall\_V4\_ext}$	$\dot{H}_{V4/amb}$	$h_{conv} = 1.42 \cdot \left(\frac{T_{V1} - T_{amb}}{L/2}\right)^{0.25}$	$S_{exch} = 0.001.m^2$	$T_{V4} - T_{amb}$

Table 4 : Convection flows.

The flow (associated with mass convection) induced by a fluid flowing with a mass flow rate $\dot{m}$, is given by the Fourier's law : $\dot{H} = \dot{m} \cdot c_p \cdot T$.

BG element	**heat flow** $\dot{H}$	**Mas flow rate** $\dot{m}$	**Specific heat** c_p	**Temperature** T
$MSf_{Hdot\_in\_PC}$	$\dot{H}_{in\_V1}$	$\dot{m}_{V1}$	$c_{p,in\_V1}(T_{in\_PC})$	T_{in_PC}
$MSf_{Hdot\_out\_PC}$	$\dot{H}_{out\_V1}$	$\dot{m}_{V1}$	$c_{p,V1}(T_{V1})$	T_{V1}
$MSf_{Hdot\_in\_SC}$	$\dot{H}_{in\_V2}$	$\dot{m}_{V2}$	$c_{p,V2}(T_{in\_SC})$	T_{in_SC}
$MSf_{Hdot\_out\_SC}$	$\dot{H}_{out\_V2}$	$\dot{m}_{V2}$	$c_{p,in\_V2}(T_{V2})$	T_{V2}

Table 5 : convection flows.

⇨ The specific heat $c_{p,liq}$ in $J/kg \cdot K$ is calculated as follows:

$$c_{p,liq} = 4709 \cdot \exp\left(-\left(\frac{T_{liq} - 583,6}{408,7}\right)^2\right) + 9669 \cdot \exp\left(-\left(\frac{T_{liq} + 48,77}{220}\right)^2\right) + 493,9 \cdot \exp\left(-\left(\frac{T_{liq} - 311,4}{109,3}\right)^2\right) \quad (17)$$

3 SIMULATION AND EXPERIMENTAL VALIDATION

The set-up presented in Figure 9 has been designed by the French company Atmostat. It represents a Mechanically Pumped Loop (2-PLMP) composed of five elements: Condenser, pipes, two-phase reservoir (TP-R), pump and an evaporator. The test bench is equipped with pressure, temperature, and flow rate sensors. The experiments have been performed in single-phase state of water.

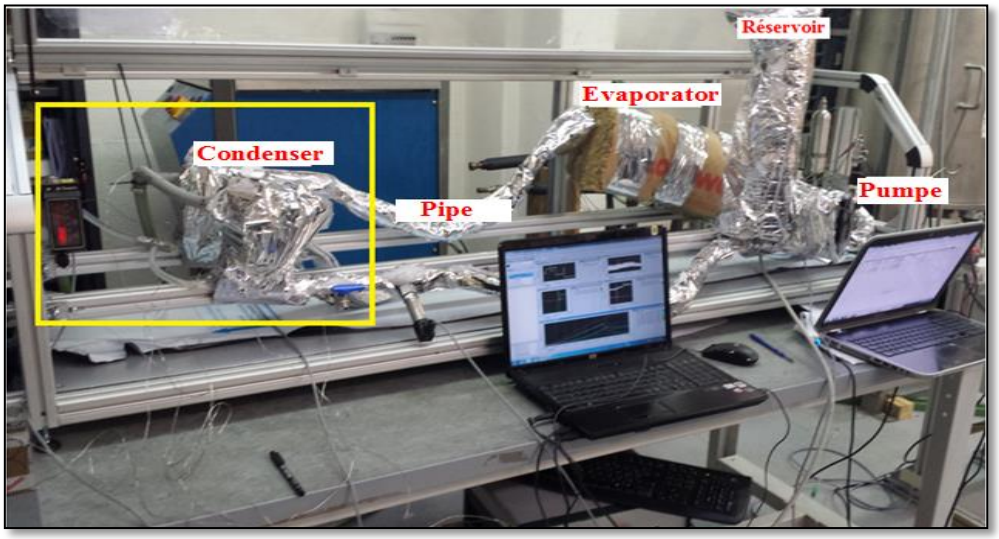

Figure 9: test bench of a mechanically pumped loop (2-PLMP).

a) Sensors distribution and strategy of the experimental validation

The Figure 10 gives a schematic representation of the BPHE with the sensors used for the experimental validation of the dynamic model.

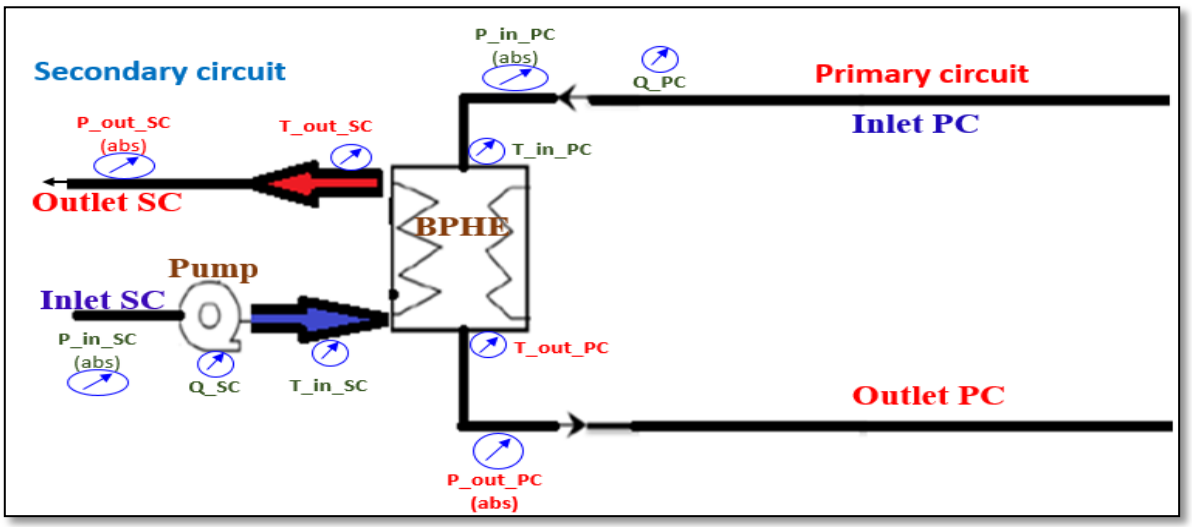

Figure 10: Distribution of pressure, temperature and volume flow rate sensors equipping the BPHE.

Legend:

P	T	Q	in	out	abs	PC	SC
pressure	Temperature	volume flow rate	Inlet	Outlet	absolute	primary circuit	secondary circuit

The set of 10 sensors shown in Figure 10 is divided into two groups:

- A first group constituted of six sensors ($Q\_PC(\exp)$, $P_{in\_PC}(\exp)$, $T_{in\_PC}(\exp)$, $P_{in\_SC}(\exp)$, $Q\_SC(\exp)$, $T_{in\_SC}(\exp)$) provides experimental data (pressure, temperature and volume flow rate) considered as inputs to launch a simulation. Corresponding time evolutions are shown in Figure 11.

- A second group of three sensors ($T_{out\_PC}(\exp)$, $T_{out\_SC}(\exp)$, $P_{out\_PC}(\exp)$) is used to validate:

1. Temperature of the liquid inside the PC noted ($T_{out\_PC}(\mathrm{mod})$) and presented Figure 11.
2. Temperature of the liquid inside the SC noted ($T_{out\_SC}(\mathrm{mod})$) and presented Figure 12.
3. Pressure of the liquid at the outlet of the PC noted ($P_{out\_PC}(\mathrm{mod})$) and presented Figure 13.

b) Geometrical data of the BPHE

All geometric features required to launch a simulation are provided by the manufacturer (SWEP) and are below recapitulated:

Parameter	notation	value	Parameter	notation	value
Number of plates	N_t	6	Volume of SC	V_{CS}	0.0741 dm3
Plate Thickness	t	0.0003 m	Volume of PC	V_{CP}	0.0494 dm3
Plate Length	L	0.154 m	Exchange surface	S_{ech}	0.048 m².
Plate Height	h	0.0174 m	material		Inox 316
Plate Width	l	0.076 m	Pitch of corrugation	p_{co}	0.001 m
Angle of chevron	β	30°	Total number of channels	$N_{can} = N_t - 1$	5

Table 6 : Summary of geometric parameters required for a simulation.

c) Discussion

Temperatures

The experimental test starts by putting into circulation the refrigerant (fluid in PC), see Figure 11 graph (c). Temperatures across the heat exchanger increase as well as the coolant (fluid in SC) is at rest, graphs (b) and (d) of Figure 11. At time 550 *s*, the coolant is launched, see Figure 11, graph (c) bleu curve. This results in a progressive decrease of temperatures across primary and secondary circuits.

The time evolutions of the liquid temperature in PC and SC, calculated by the model, show two steps clearly separated, see Figure 11 and Figure 12.

- A first step of increasing, which corresponds to the heating of the refrigerant, seems reflecting correctly the experimental temperature see Figure 11 (graph (d) curve of $T_{out\_PC}(\exp)$).
- A second step (from 550 s) of decreasing is the result of the cooling effect.

The slopes of temperature profiles in the model seem to be well transcribed. Also, the steady state, reached after 1600 *s*, is perfectly predicted by the proposed thermal hydraulic model.

The discrepancies being recorded does not exceed 1**°C,** which corresponds to the uncertainty of the thermocouples. Also, let's recall that the modeled fluid is pure water, while the fluid in the hot circuit (PC) is not really pure water but contains a certain quantity of oil: 4% of PAG.

The temperature of the liquid circulating in the (SC) is reported Figure 12 graph (d). Simulation result shows that the model predicts well the temperature of the liquid in the SC.

Furthermore, note that the validation of the thermal behavior reflects mainly the fact that thermal heat exchanges between PC, SC and the ambient are well estimated through some convection coefficients which are governing faithfully the real thermal aspect of the exchanger.

Pressure

As regards to the hydraulic behavior, Figure 13 shows finally that the mathematical correlations of pressure losses implemented in the model seem to predict well the pressure gradient along the exchanger. Note that the small increase in pressure at time 1400 *s* is due to an alteration in the mass flow rate of the primary fluid.

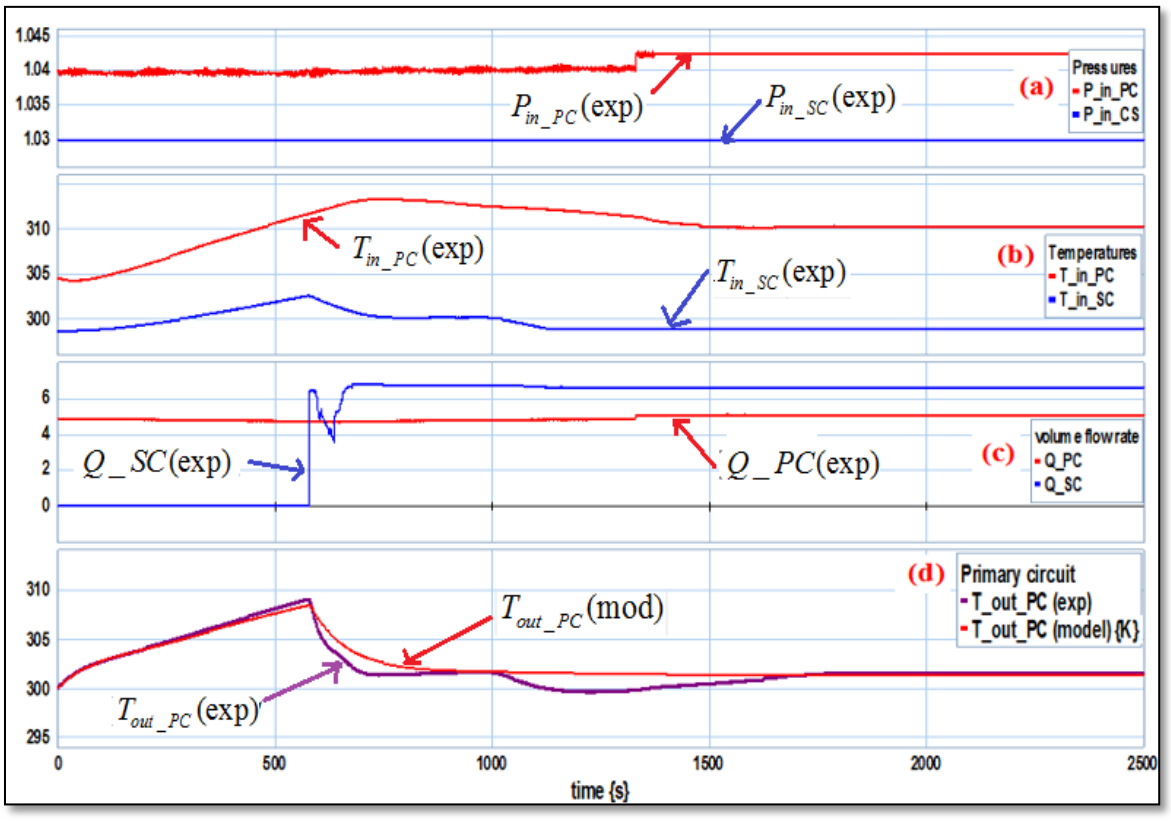

Figure 11 : Time evolution of applied solicitations (pressures, temperatures and volume flow rate) and temperature validation inside the PC.

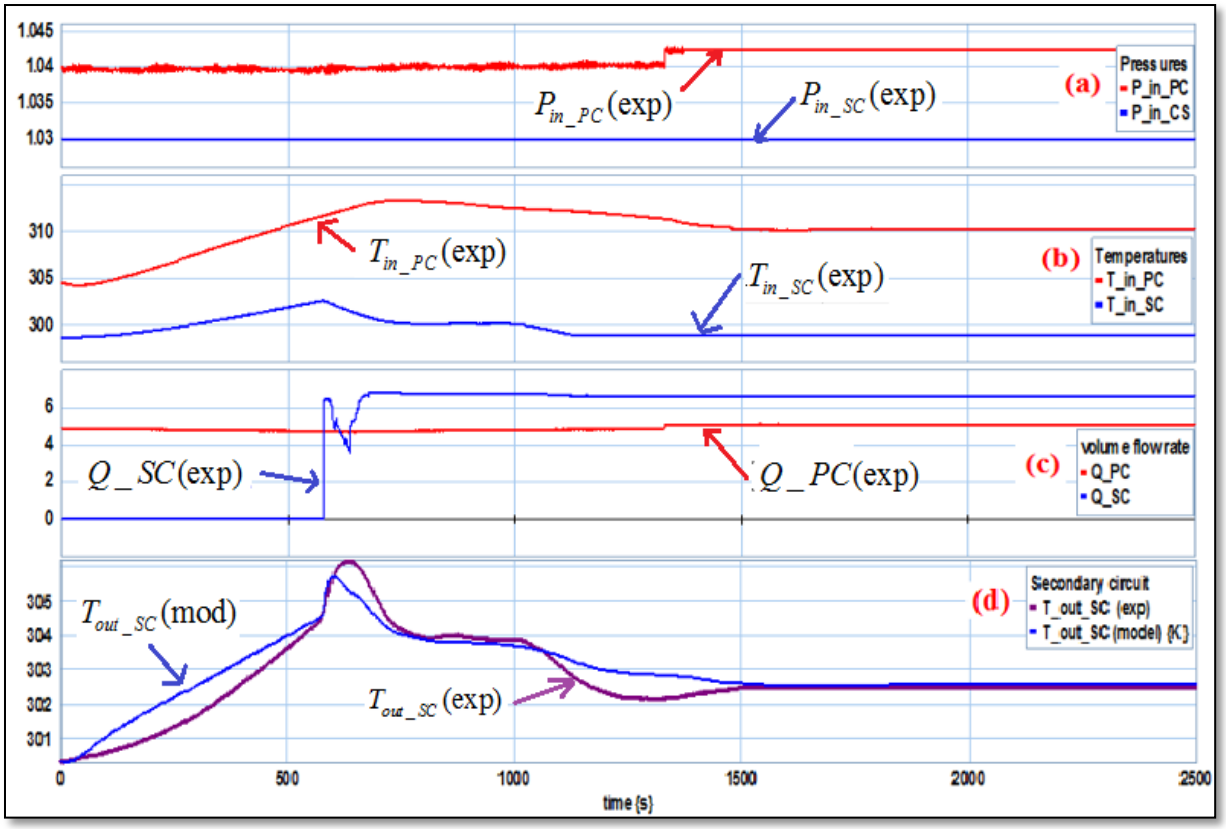

Figure 12 : Time evolution of applied solicitations (pressures, temperatures and volume flow rate) and temperature validation inside the SC.

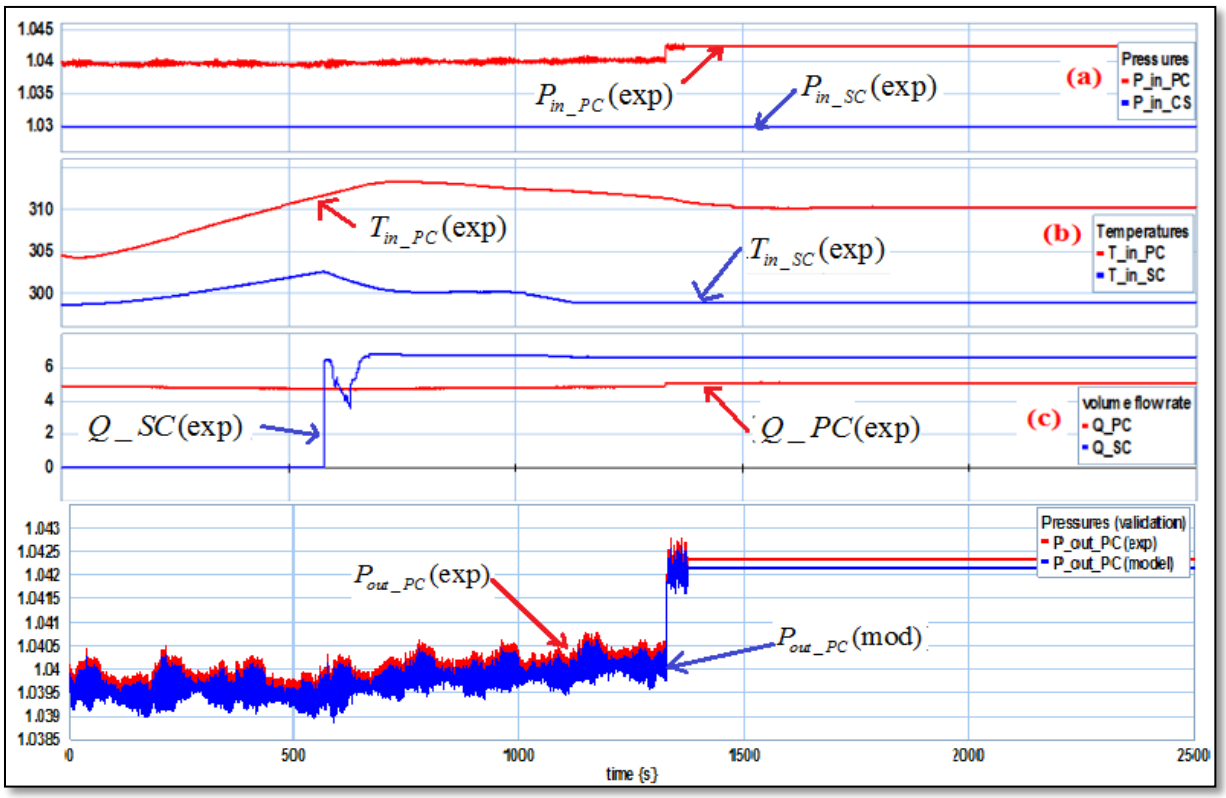

Figure 13 : Time evolution of applied solicitations and pressure validation at the outlet of the PC.

Conclusion

The article starts with a brief description of the BPHE technology. It turns out that the technology based on geometry of corrugated plates, gives the exchanger a competitive performance. This is due, in particular, to its consequent compactness and effective heat transfers. These assets have expanded the utilization of a BPHE use.

A literature review has been performed allowing the establishment of a synthesis of correlations related to thermal convection coefficients and pressure losses, classically used for monophasic flows. Then a bond graph model of the BPHE is proposed. The modularity of the bond graph approach gives the model an evolutionary aspect, where it's possible to change equations (toward a finer modeling) without changing the original structure of the model. The system is discretized into four volumes and is based on the resolution of mass and energy conservation equations. Finally, modeling of heat exchanges is realized with a noticeable attention. Indeed, the model is validated using several tests without any experimental recalibration of exchange coefficients.

Validation of the dynamic model is done by comparison of the simulation results obtained by the model and experimental data from the rig test. The objective is to evaluate the ability of the model to predict the thermo hydraulic behaviour of the fluid (water) contained in the primary circuit of the BPHE in both regimes, transitional and permanent.

References

Arman, B. & Rabas, T.J., 1995. *Condensation analysis for plate-frame heat exchangers*, Tonawanda, NY 14151-0044.

Ayub, Z.H., 2003. Plate Heat Exchanger Literature Survey and New Heat Transfer and Pressure Drop Correlations for Refrigerant Evaporators. *Heat Transfer Engineering*, (24(5)), pp.3–16.

Eldeeb, R., Radermacher, R. & Aute, V., 2014. A Model for Performance Prediction of Brazed Plate Condensers with Conventional and Alternative Lower GWP Refrigerants. In *15 th international Refrigeration and Air Conditioning Conference*. Perdue, pp. 2276–2286.

Focke W.W., Zachariades J., and O.I., 1985. Effect of the corrugation inclination angle on the thermohydraulic performance of plate heat exchangers. *International Journal of Heat and Mass Transfer*, pp.1469–1479.

Freund, S. & Kabelac, S., 2010. Investigation of local heat transfer coefficients in plate heat exchangers. *, International Journal of Heat and Mass Transfer*, vol. 53, pp.3764–3781.

Gullapalli, V.S., 2013. *Estimation of Thermal and Hydraulic Characteristics of Compact Brazed Plate Heat Exchangers Estimation of Thermal and Hydraulic Characteristics of Compact Brazed Plate Heat Exchangers*. Faculty of Engineering, LTH, Sweden.

Gut, J.A.W. et al., 2004. Thermal model validation of plate heat exchangers with generalized configurations. *Chemical Engineering Science*, 59, pp.4591–4600.

Kakac, S. & Liu, H., 1998. Heat Exchangers: Selection, Rating and Thermal Design. In *CRC Press*. New York, pp. 232– 354.

Kazuhiro, T., Toshiyuki, S., Hiroshi, T., Ktsuya, S., 2015. Bondgraphs model on cavitating pump system, International Journal of Simulation and Process Modelling, Vol. 10, Issue 2, pp. 192-203.

Kebdani, M., Dauphin-Tanguy, G., Dazin, A., Dupont, P., 2015. Bond Graph Model of a mechanically Pumped Biphasic Loop (MPBL). In *23rd Mediterranean Conference on Control and Automation*. Meliá Costa del Sol, Torremolinos, Spain.

Lachassagne, L., 2010. *Développement expérimental et modélisation numérique d ' une boucle diphasique à pompage capillaire en environnement gravitaire : application au refroidissement de composants d ' électronique de puissance en contexte automobile*. Ecole Nationale Superieure de Mecanique et d'Aerotechniquede Poitiers.

Longo, G., 2009. R410A condensation inside a commercial brazed plate heat exchanger. *Experimental Thermal and Fluid Science*, 33(2), pp.284–291. Available at: http://dx.doi.org/10.1016/j.expthermflusci.2008.09.004.

Lorenzo, C., Atharva, B. & Xiaoxiao, W., 2012. Effect of Condensation Temperature and Water Quality on Fouling of Brazed-Plate Heat Exchangers. *ASHRAE Transactions*, 118(1), pp.1086–1100.

Maqbool, M.H., 2012. *Flow boiling of ammonia and propane in mini channels*. Royal Institute of Technology. Stockholm, Sweden.

Matías, A.N, Sergio J.J., 2015. Bond-graph-based controller design for the quadruple-tank process. International Journal of Simulation and Process Modelling. Vol. 10, Issue 2, pp. 179-191.

Medjaher, K., Samantaray, A.K. & Bouamama, B.O., 2009. Bond Graph Model of a Vertical U-Tube Steam Condenser Coupled with a Heat Exchanger. *Simulation Modelling Practice and Theory*, 17, pp.228–239.

Muthuraman, S., 2011. The Characteristics of Brazed Plate Heat. *Global Journal of researches in engineering Mechanical and mechanics engineering*, 11(7), pp.11–26.

Rong, X., Kawaji, M. & Burgers, J.G., 1995. Two-phase header flow distribution in a stacked plate heat exchanger. In *Proceedings ASME/JSME FED-Gas Liquid Flows 225*. pp. 115–122.

Serin, V., 2007. *Valérie SERIN Etude hydrodynamique et thermique de la vaporisation dans un micro-canal de section carrée : application aux micro-boucles diphasiques à pompage capillaire* . UNIVERSITE TOULOUSE III - PAUL SABATIER - U.F.R. P.C.A.

Sotoodeh, A.F., Amidpour, M. & Ghaz, M., 2015. Developing of constructal theory concept for plate-fin heat exchanger modelling, design and optimisation. *International Journal of Exergy*, 18(1).

Swep, http://www.axintra.com/swep-echangueurs-a-plaques-brasees.

Taborek, J., 1992. *Shell-and-tube heat exchangers: single-phase flow, in: G.F. Hewitt (Ed.)*, B. House, ed., New York.

Thermofin, 2010. Échangeurs de chaleur à plaques brasées.

Vlasogiannis, P. et al., 2002. Air – water two-phase flow and heat transfer in a plate heat exchanger. *International Journal of Multiphase Flow*, 28(5), pp.757–772.

Volker, G. & Kabelac, S., 2010. Experimental investigations and modelling of condensation in plate heat exchangers. In Washington.

Wang, L., Sundén, B. & Manglik, R.M., 2007. Plate Heat Exchangers: Design, Applications and Performance. *WIT Press*.

[site 1] http://webbook.nist.gov/chemistry/fluid/index.html.fr